

Supporting Information

Achieving red/near-infrared mechanoresponsive luminescence turn-on: mechanically disturbed metastable nanostructures in organic solid

Kunpeng Guo,^{*a} Fang Zhang,^a Song Guo,^b Ke Li,^c Xiaoqing Lu,^c Jie Li,^{*a} Hua Wang,^a Jun Cheng,^a and Qiang Zhao^{*b}

1. Materials and Characterization

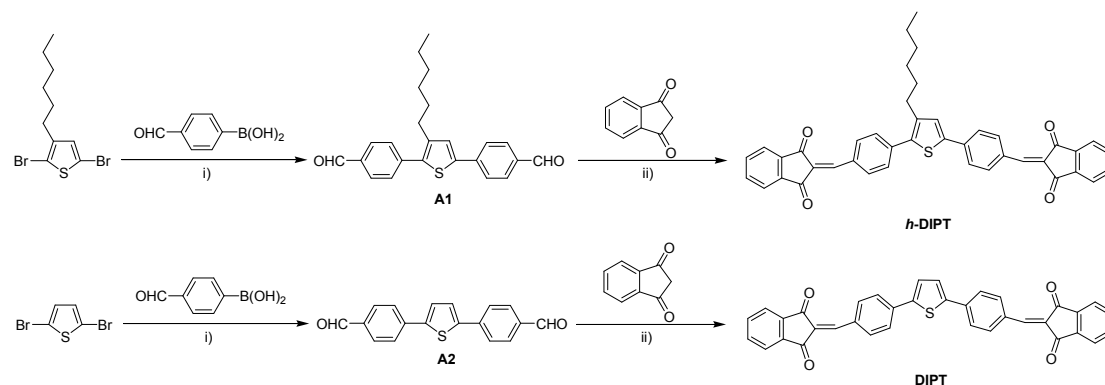
All solvents and reagents, unless otherwise stated, were of high purity quality and used as received. 1,3-Indandione, 2,5-dibromo-3-hexyl-thiophene, 4-formylbenzeneboronic acid and Pd(PPh₃)₄ were purchased from J&K Chemical.

Reactions were monitored by TLC silica plate (60F-254). NMR spectra measurements were carried out at Bruker 600 MHz for ¹H NMR and 100 MHz for ¹³C NMR, using chloroform-d as solvent. Chemical shifts were reported in parts per million (ppm) relative to internal TMS (0 ppm). Splitting patterns were described as singlet (s), doublet (d), triplet (t), quartet (q), or multiplet (m). Mass spectra measured on Microflex MALDI-TOF MS. UV-Vis spectra were recorded in a HITIACH U-3900 spectrometer. Photoluminescent (PL) spectra were recorded in a HORIBA FluoroMax-4 spectrometer. The absolute fluorescence quantum yields of solutions (10 μM) and solid powders were measured on HORIBA FluoroMax-4 by using a calibrated integrating sphere. The quartz cuvettes used were of 1 cm path length. The morphologies of the nanoaggregates were recorded on a JEM-2010F at an accelerating voltage 200 kV. The scanning electron microscopy (SEM) studies were performed using a JEOL JEM-6700F scanning electron microscope. One drop of the solution was placed on a silicon slice, which was then dried in air. Powder X-ray

diffraction (XRD) of the samples was characterized using a Philips high resolution X-ray diffraction system (model PW1825).

2. Synthesis procedures

A1 and A2 were synthesized according to literature via one step Suzuki Coupling.^[1]



Scheme S1. Synthesis of compounds ***h*-DIPT** and **DIPT**. i) Suzuki coupling, Pd(PPh₃)₄, K₂CO₃, H₂O, (CH₂OMe)₂, N₂, reflux; ii) Knoevenagel reaction, 1,3-indandione, (CH₃CH₂)₃N, CH₃COOH, CH₃CH₂OH, reflux.

2,5-Bis(4-formylphenyl)-3-hexyl-thiophene (A1). 4-Formylphenylboronic acid (720.0 mg, 4.8 mmol) was treated with 2,5-dibromo-3-hexyl-thiophene (625.1 mg, 2 mmol) in the presence of Pd(PPh₃)₄ (115 mg, 100 μmol), 1 N aqueous solution of K₂CO₃ (5 mL) and 1,2-dimethoxyethane (50 mL). The mixture was refluxed for 6 h. After cooling and addition of dichloromethane, the mixture was washed with water and dried on magnesium sulfate. Solvents were removed by rotary evaporation and the yellow black residue was purified by silica gel column chromatography with petroleum ether: EtOAc (10: 1, v:v) as eluent to afford **A1** as a yellow powder (537.6 mg, yield 71.4%). ¹H-NMR (600 MHz, CDCl₃, ppm): δ = 10.06 (s, 1H); 10.01 (s, 1H); 7.91 (d, 2H, *J* = 8.4Hz); 7.78 (d, 2H, *J* = 8.4Hz); 7.66 (d, 2H, *J* = 8.4Hz); 7.39 (s, 1H); 2.73 (t, 3H); 1.69 (m, 2H); 1.37 (m, 2H); 1.29 (m, 4H); 0.87 (t, 3H). ¹³C-NMR (150 MHz, CDCl₃, ppm): δ = 190.72; 143.25; 138.83; 134.81; 129.94; 125.46; 125.17; 31.58; 30.78; 29.32; 29.21; 22.58; 14.02. MALDI-TOF: *m/z* [M]⁺ calcd. C₂₄H₂₄O₂S, 376.1497; found: 376.1494.

***h*-DIPT.** An ethanol (20 mL) solution of compound **A1** (150.6 mg, 0.4 mmol), 1,3-indandione (145.84 mg, 1.0 mmol) and two drops of acetic acid and triethylamine

were charged sequentially into a three-necked flask and heated to reflux till no starting material **A1** was detected by the TLC plate. After cooling to room temperature, the residue was filtrated and purified by silica gel column chromatography with petroleum ether: EtOAc (10: 1, v:v) as eluent to afford **h-DIPT** as dark-red powders (220.0 mg, 86.9%). ¹H-NMR (600 MHz, CDCl₃, ppm): δ = 8.52 (d, 2H, *J* = 8.4Hz); 8.48(d, 2H, *J* = 8.4Hz); 7.99 (m, 4H); 7.86 (s, 1H); 7.80 (s, 1H); 7.79(m, 4H); 7.71 (d, 2H, *J* = 12Hz); 7.60 (d, 2H, *J* = 12Hz); 7.37 (s, 1H); 2.79 (t, 2H); 1.74 (m, 2H); 1.41 (m, 2H); 1.31 (m, 4H); 0.89 (t, 3H). ¹³C-NMR (150 MHz, CDCl₃, ppm): δ = 190.29; 190.20; 189.09; 145.91; 145.84; 142.54; 142.26; 142.03; 140.09; 139.19; 138.55; 138.39; 135.37; 135.28; 135.15; 135.08; 134.64; 132.36; 132.18; 129.08; 128.87; 128.68; 128.18; 125.36; 123.34; 123.30; 123.23; 31.65; 30.87; 29.38; 29.27; 22.62; 14.09. MALDI-TOF: m/z [M]⁺ cacl. C₄₂H₃₂O₄S, 632.2021; found:632.2019.

DIPT. A procedure similar to that for synthesizing compound **h-DIPT** was followed but using an ethanol (20 mL) solution of compound **A2** (146.2 mg, 0.50 mmol), 1,3-indandione (145.84 mg, 1.0 mmol) and two drops of acetic acid and triethylamine were charged sequentially into a three-necked flask and heated to reflux till no starting material **A2** was detected by the TLC plate. After cooling to room temperature, the residue was filtrated and washed with dichloromethane to afford **DIPT** as brown powder (286.7 mg, yield 52.3%). ¹H-NMR (600 MHz, CDCl₃, ppm): δ = 8.56 (d, 4H, *J* = 8.4Hz); 8.03 (m, 4H); 7.90 (s, 2H); 7.82(m, 8H); 7.52 (d, 2H, *J* = 12Hz). ¹³C-NMR (150 MHz, CDCl₃, ppm): δ = 190.35; 189.13; 145.88; 142.62; 142.36; 142.13; 140.13; 139.22; 138.58; 138.42; 135.41; 135.27; 134.68; 132.49; 132.31; 132.26; 129.13; 128.88; 128.74; 125.37; 123.36; 123.31; 123.24. MALDI-TOF: m/z [M]⁺ cacl. C₃₆H₂₀O₄S, 548.1082; found: 548.1079.

3. Figures

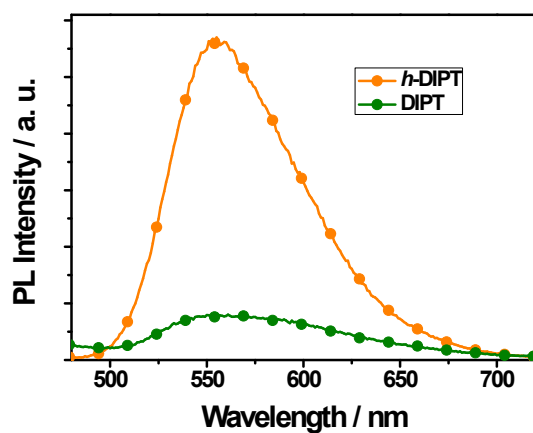


Figure S1. Fluorescent spectra of *h*-DIPT and DIPT in dilute THF solution (1×10^5 M). Excitation wavelength: 365 nm.

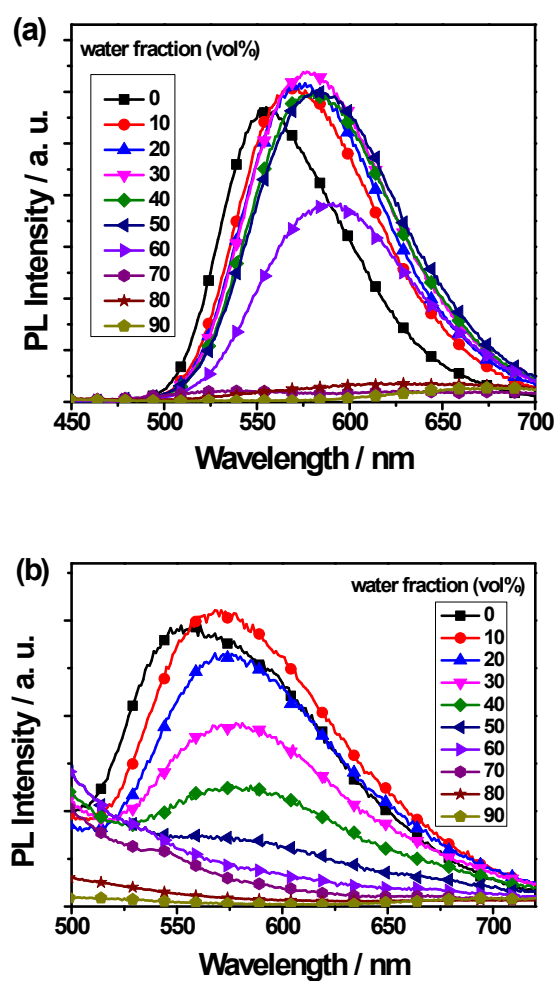


Figure S2. Fluorescent spectra of a) *h*-DIPT and b) DIPT in THF/water mixtures (1

$\times 10^5$ M) with different water fractions. Excitation wavelength: 365 nm.

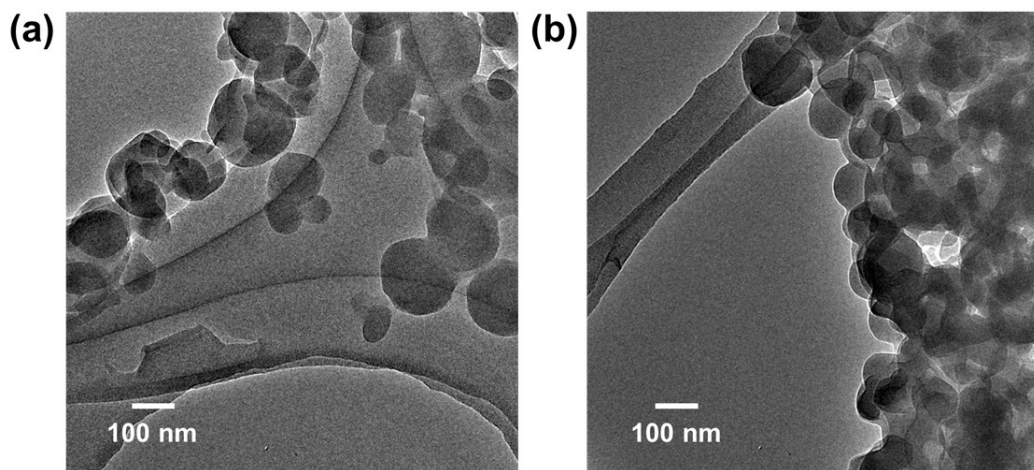


Figure S3. TEM images of a) *h*-DIPT aggregates and b) DIPT aggregates formed in 90% aqueous mixture.

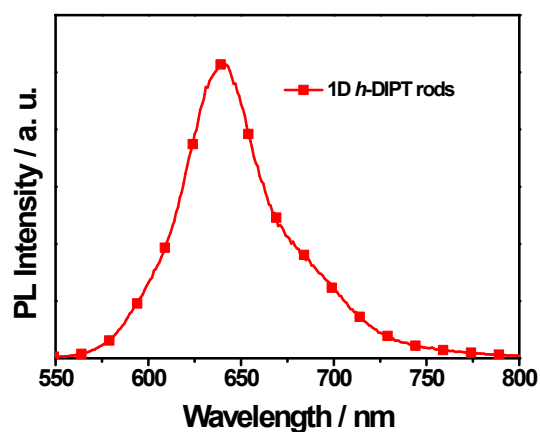


Figure S4. Fluorescent spectrum of 1D *h*-DIPT rods in solid state. Excitation wavelength: 450 nm.

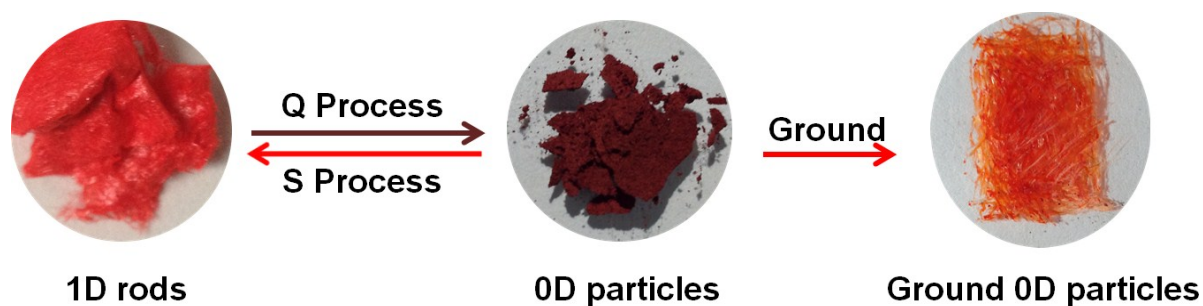


Figure S5. Images of 1D rods, 0D particles and ground 0D particles of *h*-DIPT under ambient light.

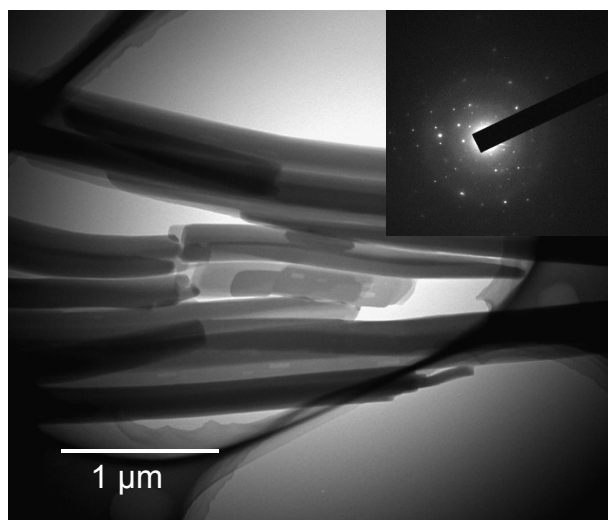


Figure S6. TEM image and SAED pattern of 1D rods of *h*-DIPT.

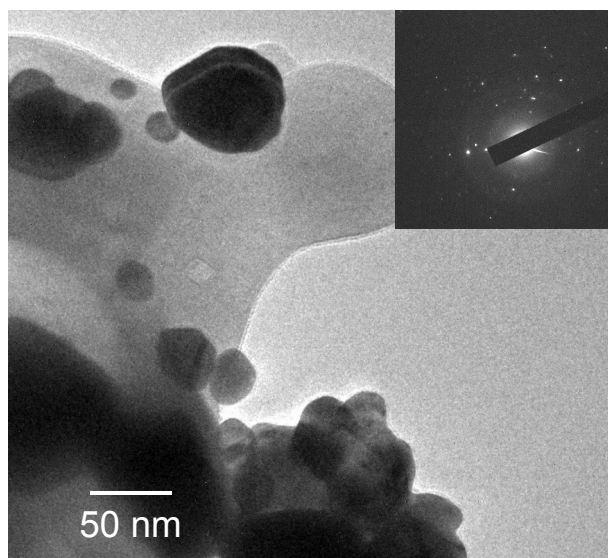


Figure S7. TEM image and SAED pattern of 0D particles of *h*-DIPT.

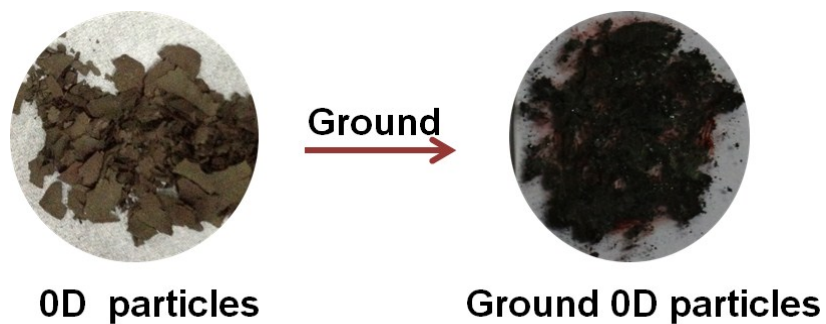


Figure S8. Images of 0D particles and ground 0D particles of **DIPT** under ambient light.

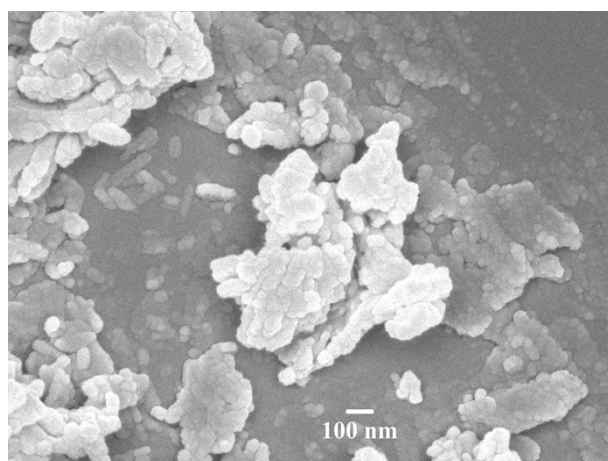


Figure S9. SEM images of 0D particles of **DIPT**.

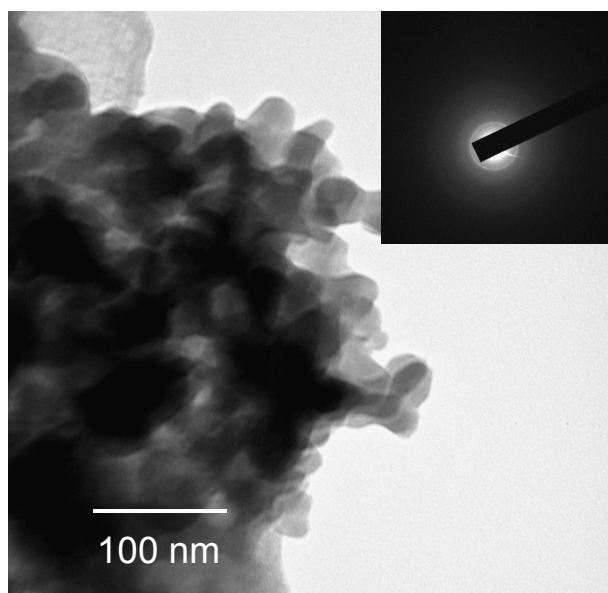


Figure S10. TEM image and SAED pattern of 0D particles of **DIPT**.

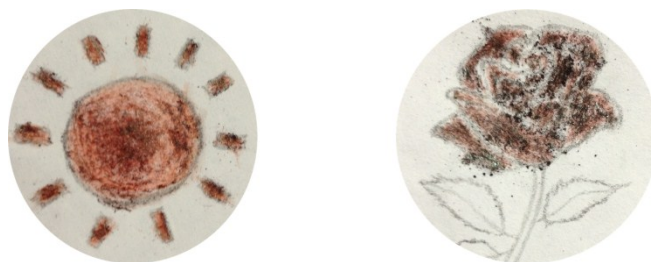


Figure S11. Images of force drawing of sun (0D particles of ***h*-DIPT**) and rose (0D particles of **DIPT**) on filter papers under ambient light.

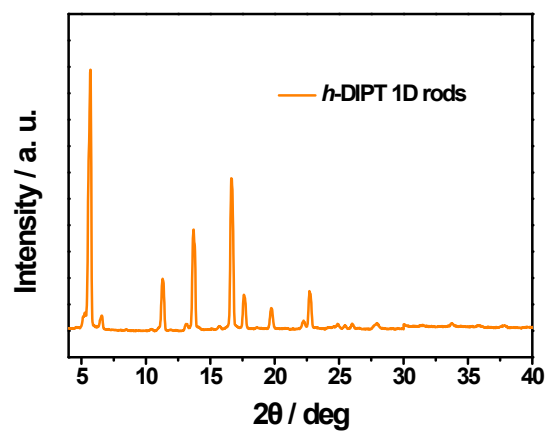


Figure S12. XRD pattern of the 1D rods of *h*-DIPT.

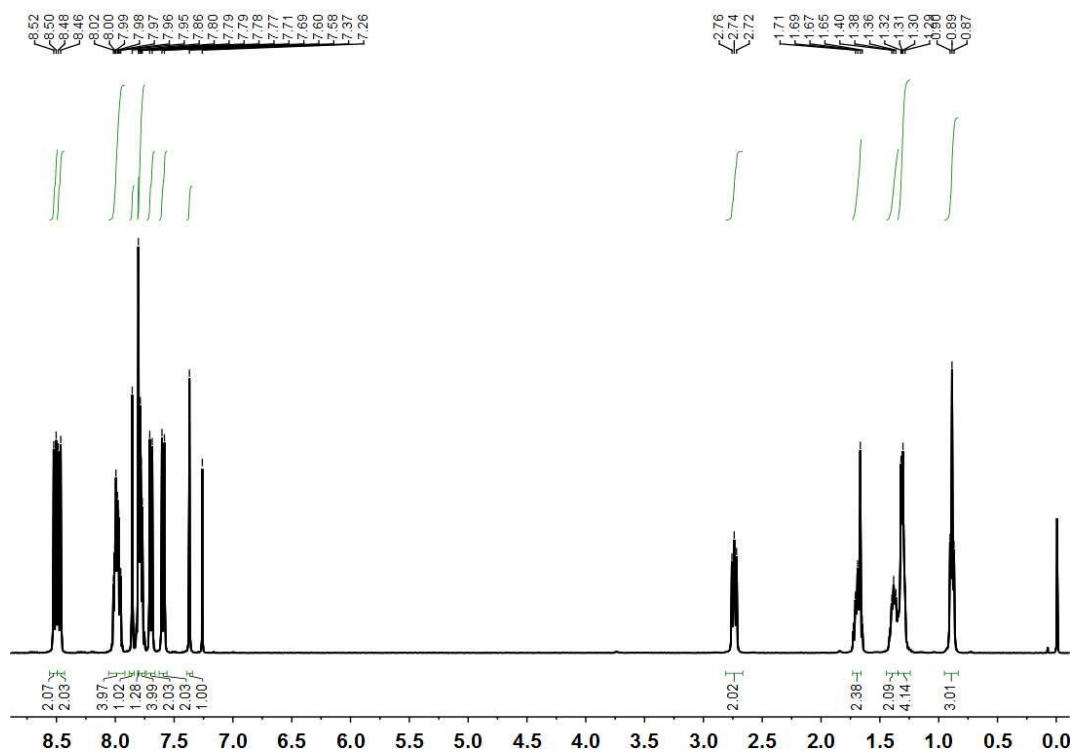


Figure S13. ^1H NMR spectrum of *h*-DIPT.

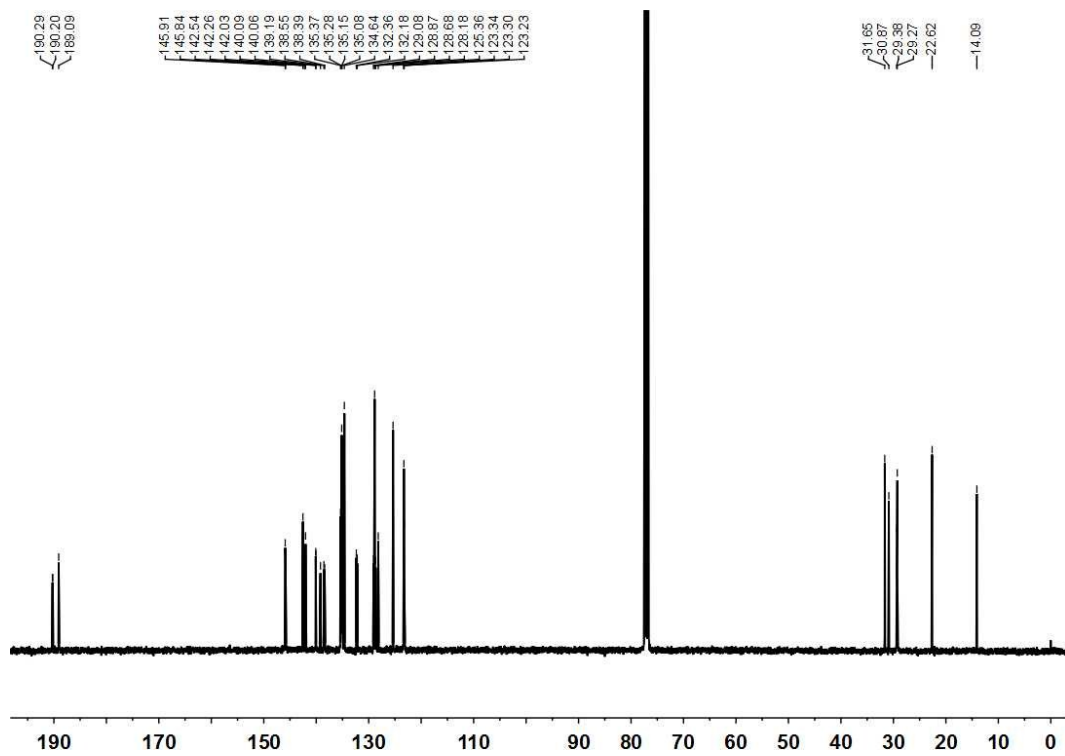


Figure S14. ^{13}C NMR spectrum of *h*-DIPT.

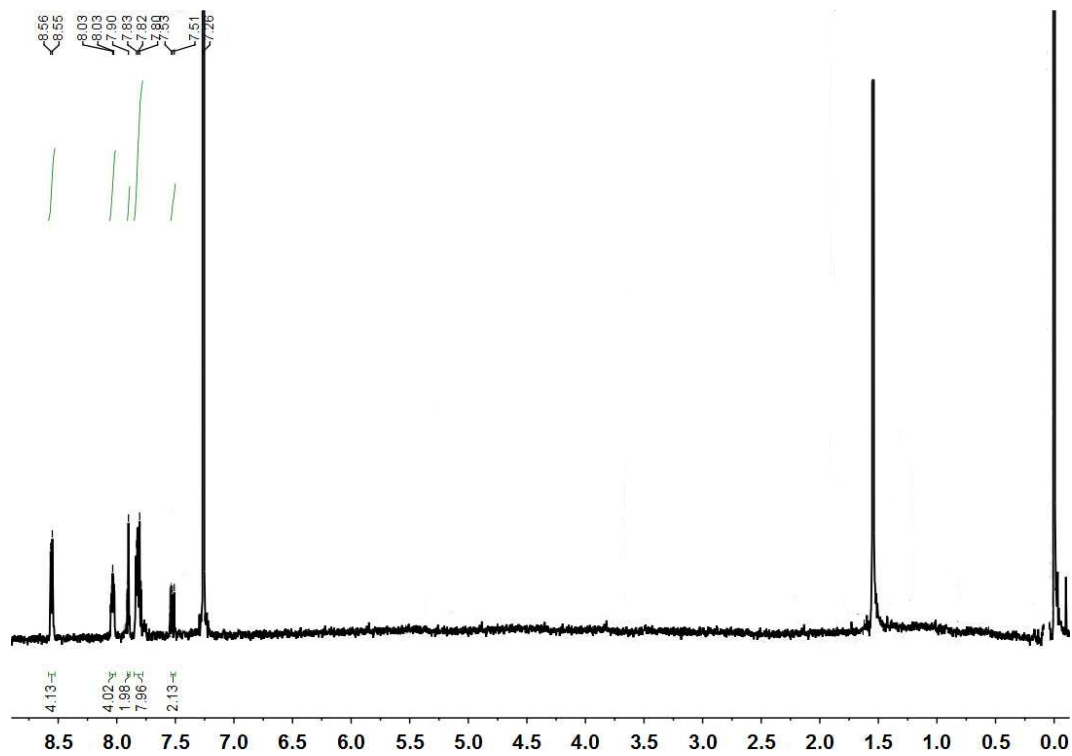


Figure S15. ^1H NMR spectrum of DIPT.

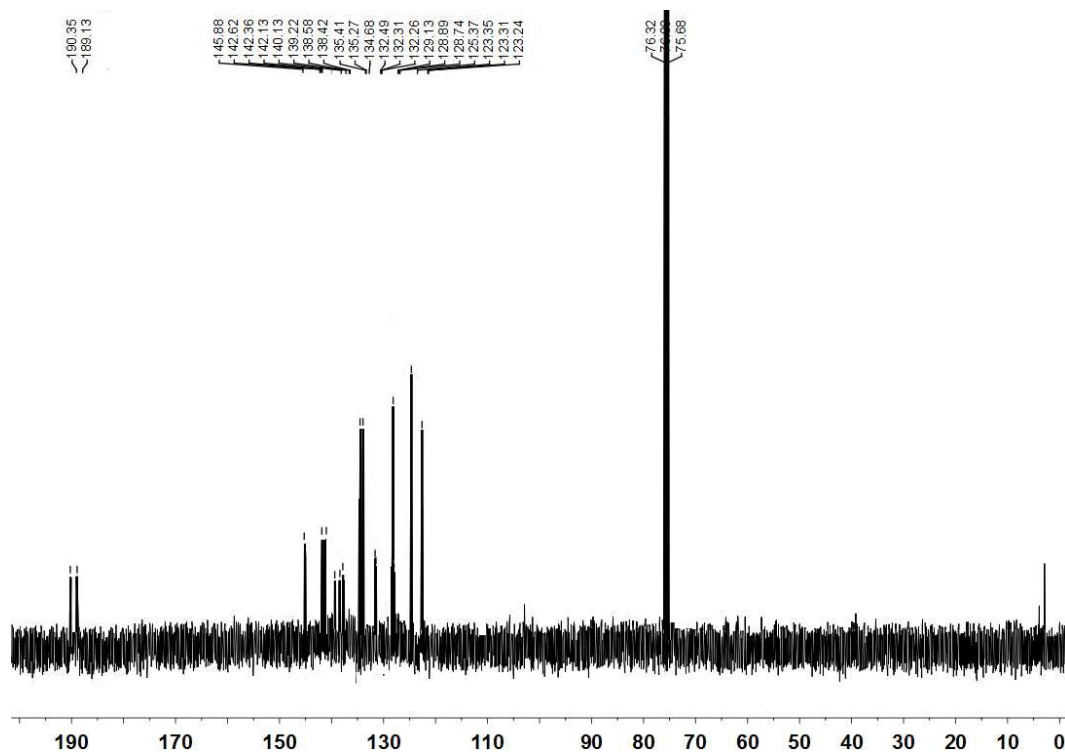


Figure S16. ^{13}C NMR spectrum of *h*-DIPT.

Reference

- [1] K. P. Guo, K. Y. Yan, X. Q. Lu, Y. C. Qiu, Z. K. Liu, J. W. Sun, F. Yan, W. Y. Guo, S. H. Yang, *Org. Lett.* **2012**, *14*, 2214.